Comparison of three measurement techniques for the normal absorption coefficient of sound absorbing materials in the free field

Kunikazu Hirosawa,[a] Kazuhiro Takashima, Hiroshi Nakagawa, Makoto Kon, and Aki Yamamoto
System Division, Nittobo Acoustic Engineering Co., Ltd., 1-21-10 Midori, Sumida-ku, Tokyo 130-0021, Japan

Walter Lauriks
Laboratorium voor Akoestiek en Thermische Fysica, Katholieke Universiteit Leuven, Celestijnenlaan 200D, BE-3001 Heverlee, Belgium

(Received 23 April 2009; revised 3 September 2009; accepted 7 September 2009)

Three different techniques for evaluating the absorption coefficient of sound absorbing materials in free field conditions are discussed. One technique measures the acoustic impedance at one point nearby a specimen, the other two techniques evaluate the impedance from the transfer function of two sound pressures and two particle velocities at two points. These are called "PU-method," "PP-method," and "UU-method," respectively. An iterative algorithm to estimate the acoustic impedance of the locally reactive specimen in the spherical wave field is also applied. First, the effect of receiver positions, specimen areas, and source heights to the measured normal absorption coefficient is investigated by the boundary element method. According to these investigations, the PU-method is most stable against the effect of specimen area, and the UU-method is easily affected by that effect. Closer source to the specimen distance is advantageous for the signal to noise ratio of these measurement techniques, but correction for the effect of the spherical wave field has to be applied. As a finding, the iterative algorithm works for all of three techniques. Finally, the PU-method is applied experimentally with a pressure-velocity sensor and a loudspeaker in a hemi-anechoic room. As a result, the calculated results have been verified.
 [DOI: 10.1121/1.3242355]

PACS number(s): 43.55.Ev, 43.58.Bh, 43.20.El, 43.20.Rz [NX] Pages: 3020–3027

I. INTRODUCTION

There are several methods to measure the absorption coefficient or the acoustic impedance of acoustical materials. The method with impedance tubes[1] may generally be used for the normal incident absorption coefficient and the acoustic impedance. The method has advantages that a specimen can be small and, especially for the transfer-function method, the measuring time is short. In this method, however, the dimensions of the impedance tubes limit the frequency range, and a specimen needs to be cut carefully from an original absorbing material. Moreover, the measured results of the large material block itself and of the small cut specimen tend to differ when the specimen is a poroelastic material.[2]

Measurement methods in the free field[3–8] have a possibility to overcome the mentioned problem. Since a specimen does not need to be cut out from an original material in the free field methods, it can be used to measure the essential properties of a material regardless of the specimen size. A typical method is called the transfer function method using the sound pressures at two microphones.[5–7] Recently a new PU-probe was developed,[9] it can measure the sound pressure and the particle velocity simultaneously at the same point. Measurement methods with PU-probe have been developed;[10,11] the acoustic impedance at one point nearby the specimen is measured by this method. Some of the free field methods use a plane-wave hypothesis that the field around the receiver positions is assumed to be a plane-wave field. In actual situation, the field around the receivers is better approximated as a spherical wave field, especially at low frequencies. The reflection factor should be calculated by the method taking the spherical wave field into account.[12] However, it cannot be estimated by the direct measurement or calculation because the spherical wave field solution needs the acoustic impedance of the specimen or the reflection coefficient for the plane wave. They are the values to be identified, nevertheless, to estimate the values; the solutions of the spherical wave field model are required. This contradiction can be resolved by an iterative determination algorithm[7,11] which estimates the acoustic impedance of the specimen iteratively. Therefore, the reflection coefficient, the acoustic impedance, or the absorption coefficient of the specimen is estimated by the iterative determination.

The edge effect of a specimen or unwanted reflected waves from wedges of an anechoic room or reflection objects can affect the values measured by these free field methods. To avoid that, it can be expected that a measurement using the particle velocity has robustness against these effects. Be-

[a]Author to whom correspondence should be addressed. Electronic mail: hirosawa@noe.co.jp.

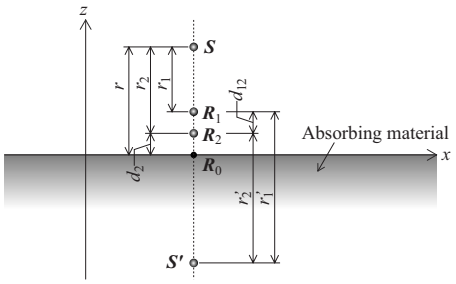

FIG. 1. Illustration of the setup for three measurement techniques. Here, $\boldsymbol{S}$ is the real point source, $\boldsymbol{S}'$ is the imaginary point source, $\boldsymbol{R}_1$ and $\boldsymbol{R}_2$ are receiver points, and $\boldsymbol{R}_0$ is the intersection of the line $\boldsymbol{R}_1\boldsymbol{R}_2$ with the surface of the absorbing material.

cause the particle velocity is a vector and the normal component for a specimen can be considered to be robust against the effect from the other directions. Therefore, the new measurement technique can be considered to use the particle velocities at two points. In this paper, three measurement techniques in the free field, which are measurements of two sound pressures by two microphones, a sound pressure and a particle velocity by PU-probe, and two particle velocities by two velocity sensors, are compared with regard to *in-situ* measurement technique of the normal absorption coefficient. Here, the measurement using two sound pressures is called "PP-method," the measurement using a sound pressure and a particle velocity is called "PU-method," and the measurement using two particle velocities is called "UU-method." First, the edge effect caused by various sizes of the specimen, the sound source heights, and the receiver positions to the normal absorption coefficient are investigated by the boundary element method (BEM) instead of physical experiments. Then, the PU-method is investigated by some experiments. The iterative determination algorithm based on the method proposed by Allard and Champoux[7] is applied to all results of PP-, PU-, and UU-methods on these investigations.

In this paper, the angular frequency is expressed as ω, time is t, the imaginary unit is $j=\sqrt{-1}$, and all time-varying quantities should obey the time dependence $\exp(-j\omega t)$.

II. MEASUREMENT TECHNIQUES

Figure 1 shows the setup for examining three measurement techniques. r_1 is the distance between $\boldsymbol{S}$ and $\boldsymbol{R}_1$, r_2 is $\boldsymbol{S}$ and $\boldsymbol{R}_2$, r_1' is $\boldsymbol{S}'$ and $\boldsymbol{R}_1$, r_2' is $\boldsymbol{S}'$ and $\boldsymbol{R}_2$, and r is $\boldsymbol{S}$ and $\boldsymbol{R}_0$, respectively. d_{12} is the distance between $\boldsymbol{R}_1$ and $\boldsymbol{R}_2$, and d_2 is $\boldsymbol{R}_2$ and $\boldsymbol{R}_0$. The three measurement techniques are assumed that the absorbing material has a locally reacting surface.

A. PU-method

In Fig. 1, $\boldsymbol{R}_2$ is the receiver position for this method. Since the specific acoustic impedance $Z_n(\boldsymbol{R}_2)$ is the ratio of the sound pressure $p(\boldsymbol{R}_2)$ and the $-z$ directional particle velocity $u_n(\boldsymbol{R}_2)$, the plane-wave reflection coefficient R_p is given by[10]

$$R_p = \frac{\dfrac{e^{jkr_2}}{r_2}}{\dfrac{e^{jkr_2'}}{r_2'}} \cdot \frac{Z_n(\boldsymbol{R}_2)\dfrac{1-jkr_2}{jkr_2} - \rho c}{Z_n(\boldsymbol{R}_2)\dfrac{1-jkr_2'}{jkr_2'} + \rho c}, \tag{1}$$

where ρ is the density of air, c is the sound speed in air, and $k=\omega/c$ is the wave number.

B. PP-method

The plane-wave reflection coefficient R_p is given by[7]

$$R_p = \frac{\dfrac{e^{jkr_2}}{r_2} - H(\omega)\dfrac{e^{jkr_1}}{r_1}}{H(\omega)\dfrac{e^{jkr_1'}}{r_1'} - \dfrac{e^{jkr_2'}}{r_2'}}, \tag{2}$$

where $H(\omega)=p(\boldsymbol{R}_2)/p(\boldsymbol{R}_1)$ is the transfer function between the sound pressures at receivers $\boldsymbol{R}_1$ and $\boldsymbol{R}_2$.

C. UU-method

The plane-wave reflection coefficient R_p is given by

$$R_p = \frac{\dfrac{1-jkr_2}{r_2}\dfrac{e^{jkr_2}}{r_2} - H'(\omega)\dfrac{1-jkr_1}{r_1}\dfrac{e^{jkr_1}}{r_1}}{\dfrac{1-jkr_2'}{r_2'}\dfrac{e^{jkr_2'}}{r_2'} - H'(\omega)\dfrac{1-jkr_1'}{r_1'}\dfrac{e^{jkr_1'}}{r_1'}}, \tag{3}$$

where $H'(\omega)=u_n(\boldsymbol{R}_2)/u_n(\boldsymbol{R}_1)$ is the transfer function between the $-z$ directional particle velocities at receivers $\boldsymbol{R}_1$ and $\boldsymbol{R}_2$.

D. Iterative determination algorithm

The plane-wave reflection coefficient R_p in Eqs. (1)–(3) is derived from the assumptions that a distance between a source and a receiver is very long and a field around a receiver is regarded as the plane-wave field approximately. However, these assumptions are not correct especially in the low frequencies, and the reflection coefficient R_p for the plane wave estimated by Eqs. (1)–(3) is not valid. R_p should be estimated for the spherical wave field; nevertheless R_p cannot be estimated by direct measurement or calculation using Eqs. (1)–(3). Because estimating the reflection coefficient for the spherical wave needs the reflection coefficient for the plane wave which is unknown and is the value to be identified. In this paper, this discrepancy is resolved by the iterative determination algorithm based on the method proposed by Allard and Champoux.[7] The method can iteratively obtain the acoustic impedance Z_n of a specimen from the reflection coefficient R_p directly estimated by Eqs. (1)–(3), and then the reflection and absorption coefficients are calculated from Z_n. Ingard's[13] exact solution is applied to the spherical field solution in this algorithm.

1. Ingard's exact solution

Figure 2 shows the geometry of the sound propagation above the infinite plane with the finite specific acoustic impedance Z_n. r_1 is the distance between $\boldsymbol{S}$ and $\boldsymbol{R}_1$, r_1' is the distance between $\boldsymbol{S}'$ and $\boldsymbol{R}_1$, and the angle Θ is defined as the

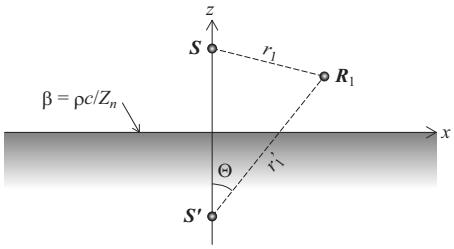

FIG. 2. Geometry of the sound propagation above an infinite plane with a finite acoustic impedance. Here, $\boldsymbol{S}$ is the real point source, $\boldsymbol{S}'$ is the imaginary point source, and $\boldsymbol{R}_1$ is receiver point.

line $\boldsymbol{S}$,$\boldsymbol{R}_1$ and the z axis. $\beta=\rho c/Z_n$ is the normalized specific acoustic admittance of the locally reacting infinite plane. According to Ingard's[13] exact solution, the velocity potential $\varphi(\boldsymbol{R}_1)$ is given by

$$\varphi(\boldsymbol{R}_1)=\frac{e^{jkr_1}}{r_1}+\{R_p+(1-R_p)F\}\frac{e^{jkr_1'}}{r_1'},$$

$$F=1-(\beta+\gamma_0)(kr_1')\times\int_0^\infty\frac{e^{-kr_1's}ds}{\sqrt{(1+\beta\gamma_0+js)^2-(1-\gamma_0^2)(1-\beta^2)}},$$

$$\gamma_0=\cos\Theta,\quad R_p=(\gamma_0-\beta)/(\gamma_0+\beta), \tag{4}$$

where R_p is the plane-wave reflection coefficient of the infinite plane.

The sound pressure $p(\boldsymbol{R}_1)$ and the particle velocity $u(\boldsymbol{R}_1)$ are given by

$$p(\boldsymbol{R}_1)=\rho\frac{\partial\varphi(\boldsymbol{R}_1)}{\partial t}, \tag{5}$$

$$u(\boldsymbol{R}_1)=-\operatorname{grad}\varphi(\boldsymbol{R}_1). \tag{6}$$

Since the normal incidence is considered in this paper, Eq. (4) essentially means the same as the solution for perpendicular incidence according to Nobile and Hayek,[14] and only expressions for both solutions are different when $\gamma_0=1$ in Eq. (4). Champoux and L'Espérance[5] discussed the gradient of the velocity potential developed by Nobile and Hayek that describes the particle velocity in the spherical wave field above the locally reacting impedance plane. The gradient of F in Eq. (4) can be derived from the same way as Champoux and L'Espérance.[5] In this paper, the integrals in Eq. (4) and the gradient of F are computed by the Gauss–Legendre quadrature with discretized integral intervals. Even though these integrations are from zero to infinity, these integrands $f(s)$ can converge at zero with $s\to\infty$. Therefore, the truncated upper bound U of these integrals can be introduced, and it can be estimated with the following condition:

$$\left|\int_0^U f(s)ds-\int_0^{U+\Delta U}f(s)ds\right|\Big/\left|\int_0^U f(s)ds\right|\le C, \tag{7}$$

where ΔU is the discretized integral interval and $C=10^{-13}$ in this paper.

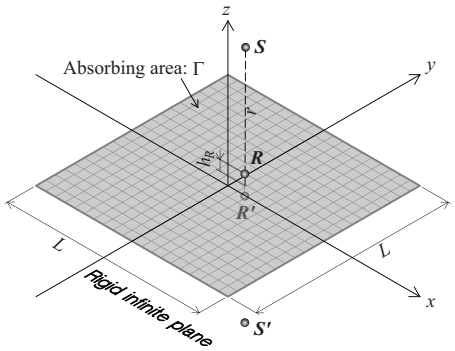

FIG. 3. Illustration of the boundary element analysis model. Here, $\boldsymbol{S}$ is the real point source, $\boldsymbol{S}'$ is the imaginary point source, $\boldsymbol{R}$ is the receiver point, and h_R is the receiver height.

2. Iterative procedure

The iterative determination algorithm is as follows

(1) The normal acoustic impedance $Z_n^{(0)}$ $(i=0)$ at $\boldsymbol{R}_0$ in Fig. 1 is estimated by the following equation substituting R_p given by Eqs. (1)–(3):

$$Z_n^{(i)}=\frac{\rho c(1+R_p)}{(1-R_p)(1-1/jkr)}. \tag{8}$$

Since $Z_n^{(0)}$ is obtained from the measured values, it is used as the reference value in this algorithm. i is the iterative index.

(2) $Z_n^{(0)}$ is set as the initial value of the desired normal specific acoustic impedance Z_n of the absorbing material surface, viz., $Z_n=Z_n^{(0)}$.

(3) Z_n is substituted for Eq. (4), and the sound pressures and the particle velocities at $\boldsymbol{R}_1$ and $\boldsymbol{R}_2$ are calculated through Eqs. (5) and (6).

(4) In order to estimate R_p, $Z_n(\boldsymbol{R}_2)=p(\boldsymbol{R}_2)/u(\boldsymbol{R}_2)$ in PU-method is substituted for Eq. (1), $H(\omega)=p(\boldsymbol{R}_2)/p(\boldsymbol{R}_1)$ in PP-method is substituted for Eq. (2), or $H'(\omega)=u_n(\boldsymbol{R}_2)/u_n(\boldsymbol{R}_1)$ in UU-method is substituted for Eq. (3).

(5) $Z_n^{(i)}$ is calculated by Eq. (8) substituting R_p.

(6) It is judged that whether $Z_n^{(i)}$ is equal to $Z_n^{(0)}$ or not. If $Z_n^{(i)}\neq Z_n^{(0)}$, go to (7). Otherwise, go to (8).

(7) Z_n is corrected by the following equation:

$$Z_n=Z_n+Z_n^{(i)}-Z_n^{(0)}. \tag{9}$$

Returning to (3), and the updated Z_n is substituted for Eq. (4) again. The above procedure is repeated until $Z_n^{(i+1)}$ is equal to $Z_n^{(0)}$.

(8) The plane-wave reflection coefficient and the absorption coefficient of the absorbing material are estimated from Z_n determined by this algorithm.

In this paper, the convergence condition of (6) in the iterative procedure is that the relative error between $Z_n^{(i)}$ and $Z_n^{(0)}$ is less than 10^{-6}.

III. NUMERICAL INVESTIGATION WITH BEM

A. Analysis model

Figure 3 shows three-dimensional hemi-free field; x-y plane is the rigid infinite plane. There is the absorbing area Γ

which has L (m) $\times L$ (m) area, and the center of the absorbing area is set to the origin. The distance between $\boldsymbol{S}$ and Γ is r (m), and the height of $\boldsymbol{R}$ from Γ is h_R (m).

The mirror image method is applied to the analysis model, and Γ is modeled as a locally reacting plane with the normal specific acoustic impedance Z_n. The Helmholtz–Huygens integral of the sound pressure $p(\boldsymbol{R})$, which describes the sound field, can be written as follows:[15,16]

$$p(\boldsymbol{R}) = G(\boldsymbol{S},\boldsymbol{R}) + G(\boldsymbol{S}',\boldsymbol{R}) + \frac{2jk\rho c}{Z_n}\int\int_{\Gamma} p(\boldsymbol{r}_\Gamma)G(\boldsymbol{r}_\Gamma,\boldsymbol{R})d\Gamma, \quad (10)$$

where G is the Green's function in the three-dimensional free field, and $\boldsymbol{r}_\Gamma$ is an arbitrary point on Γ. When $\boldsymbol{R}$ is on Γ, Eq. (10) becomes the Fredholm integral equation of the second kind which has unknown values $p(\boldsymbol{r}_\Gamma)$. The solutions are obtained by solving the linear simultaneous equations after discretization of Γ into boundary elements. The boundary element is quadrilateral constant element and the maximum element length is less than 1/8 wavelength at the frequency.

In this paper, the absorbing area Γ is assumed to be a glass wool with thickness of 25 mm (flow resistivity of 55 000 N s/m^4), and Z_n of Γ is estimated by the empirical equation proposed by Allard and Champoux.[17]

The whole edge effect should be considered with this formulation of the BEM in frequency domain.

B. Effect of receiver positions

To investigate the normal absorption coefficient affected by the effect of receiver positions, the sound pressures and the particle velocities at four receiver points $\boldsymbol{R}_2^{(1)}=(0,0,0.01)$, $\boldsymbol{R}_2^{(2)}=(0.1,0,0.01)$, $\boldsymbol{R}_2^{(3)}=(0.1,0.1,0.01)$, and $\boldsymbol{R}_2^{(4)}=(0.1,0.05,0.01)$ with $d_{12}=0.01$ m are calculated by the BEM. The distance r is fixed at 1.0 m, and the absorbing area Γ is 1.0×1.0 m^2.

Figure 4(a) shows the normal absorption coefficient estimated by the PU-method, Fig. 4(b) shows that by the PP-method, and Fig. 4(c) shows that by the UU-method, respectively.

The legend "TMM" in these figures describes the normal absorption coefficient calculated by the transfer matrix method[18] (TMM) using the material characteristics. The propagation constant and the characteristic impedance in the TMM are also estimated by the empirical equation of Allard and Champoux.[17] The situation supposed in the TMM is that a plane wave propagates into an absorbing material with infinite area, and the edge effect is not considered. Therefore, the normal absorption coefficient calculated by the TMM is the reference value on the numerical investigation in this paper.

From these results, differences of the normal absorption coefficient caused by different receiver positions are found. The differences can be caused by the diffracted waves from the edges of the absorbing area Γ, and especially $\boldsymbol{R}^{(1)}$ is the center of Γ, and the diffracted waves equally affect the sound pressure and the particle velocity at $\boldsymbol{R}^{(1)}$ in phase. In contrast, the effect of the diffracted waves at $\boldsymbol{R}^{(4)}$ is dispersed as a result of the different distances between the edges and $\boldsymbol{R}^{(4)}$, and these figures also indicate that the values at $\boldsymbol{R}^{(4)}$ are most stable. Therefore, the receiver positions of these measurement techniques should not be set to the center. In what follows, the normal absorption coefficient at $\boldsymbol{R}^{(4)}$ is investigated.

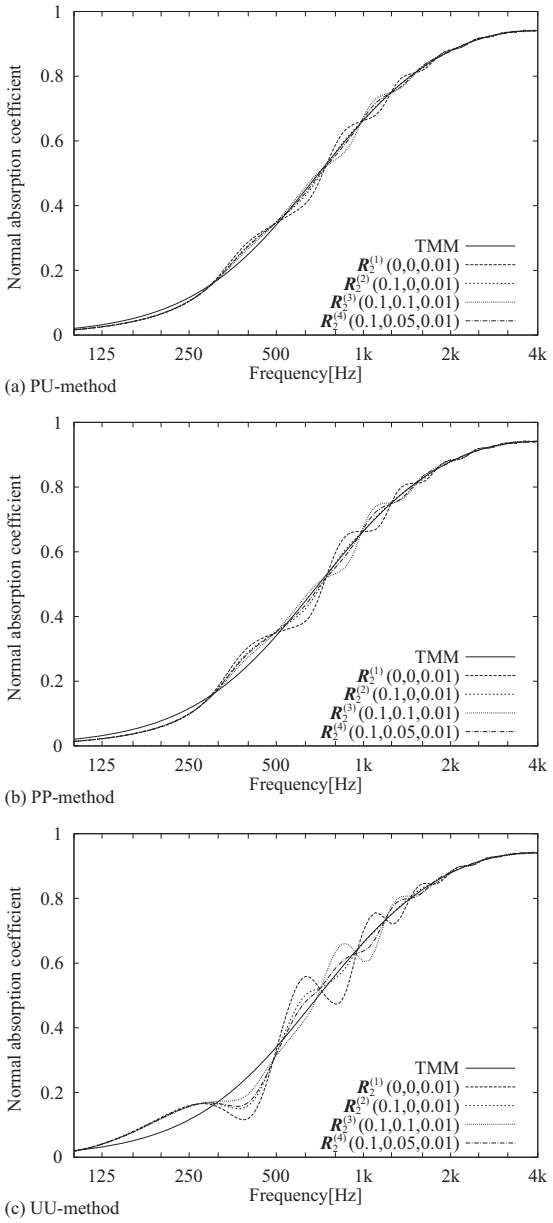

FIG. 4. Comparison of the normal absorption coefficients calculated by the BEM: r is 1.0 m and Γ is 1.0×1.0 m^2. Effect of receiver positions: (a) is estimated by the PU-method, (b) by the PP-method, and (c) by the UU-method.

C. Effect of absorbing areas

The normal absorption coefficient estimated by the PU-method is shown in Fig. 5(a), that by the PP-method in Fig. 5(b), and that by the UU-method in Fig. 5(c), respectively. Compared absorbing areas are 0.25×0.25, 0.5×0.5, 1.0×1.0, 2.0×2.0, and 3.0×3.0 m^2. Positions are $\boldsymbol{S}=(0.1,0.05,1.0)$, $\boldsymbol{R}_1=(0.1,0.05,0.02)$, and $\boldsymbol{R}_2=(0.1,\ 0.05,\ 0.01)$, and the distance r is 1.0 m.

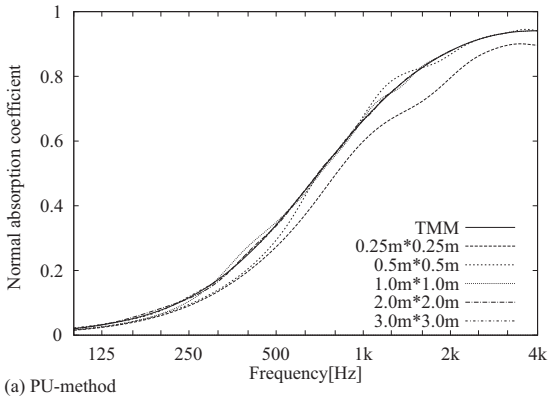

(a) PU-method

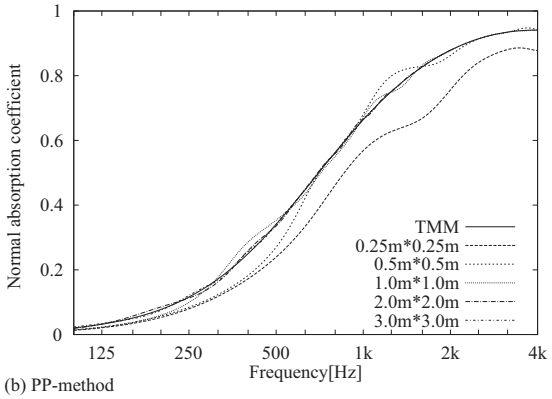

(b) PP-method

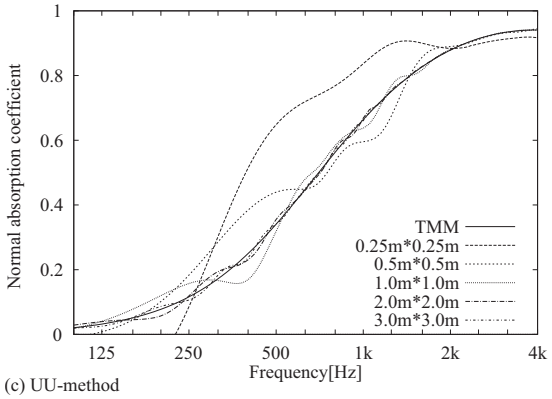

(c) UU-method

FIG. 5. Comparison of the normal absorption coefficients calculated by the BEM: r is 1.0 m. Effect of absorbing areas: (a) is estimated by the PU-method, (b) by the PP-method, and (c) by the UU-method.

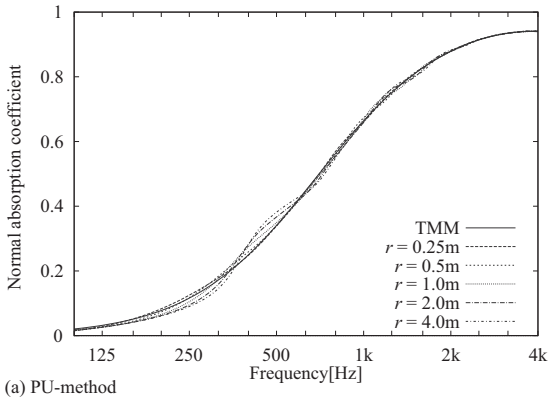

(a) PU-method

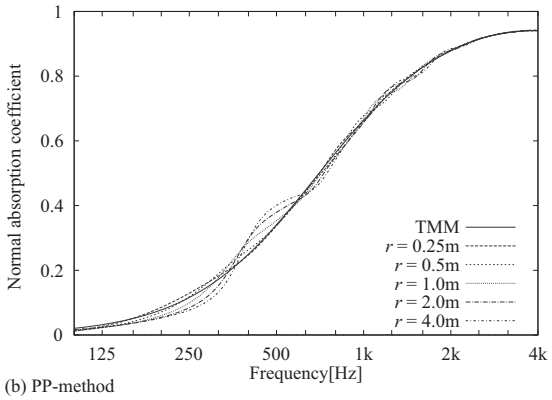

(b) PP-method

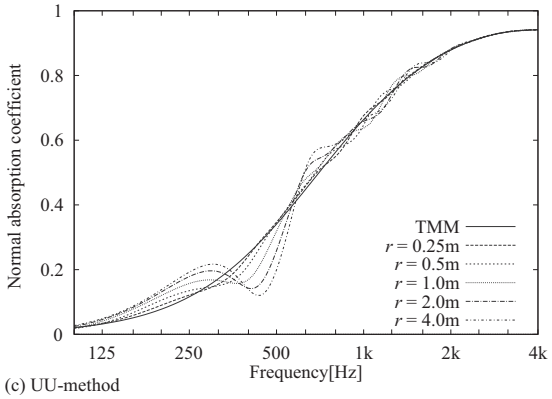

(c) UU-method

FIG. 6. Comparison of the normal absorption coefficients calculated by the BEM: Γ is 1.0×1.0 m^2. Effect of source heights: (a) is estimated by the PU-method, (b) by the PP-method, and (c) by the UU-method.

The frequency characteristic of the normal absorption coefficient of the PU-method is very similar to that of the PP-method; however, that of the PP-method is slightly more deviated than that of the PU-method. On the other hand, that of the UU-method differs from those of the PU- and the PP-methods, and it is more deviated than the others. The normal absorption coefficient of the three techniques tends to converge at that of the TMM when the area becomes larger. Therefore, it is found that the PU-method is most robust against the effect of absorbing areas in the three measurement techniques. In addition, the area has to be larger than 1.0×1.0 m^2 in the case of the PU-method.

D. Effect of source heights

The normal absorption coefficient estimated by the methods of the PU, the PP, and the UU is compared on the different distances of the source height r=0.25, 0.5, 1.0, 2.0, and 4.0 m. Figure 6(a) shows the normal absorption coefficient estimated by the PU-method, Fig. 6(b) shows that by the PP-method, and Fig. 6(c) shows that by the UU-method. The positions are $\boldsymbol{S}=(0.1,0.05,r)$, $\boldsymbol{R}_1=(0.1,0.05,0.02)$, and $\boldsymbol{R}_2=(0.1,0.05,0.01)$, and the absorbing area is 1.0×1.0 m^2.

In all three measurement techniques, if $\boldsymbol{S}$ is closer to the sample surface Γ, the normal absorption coefficient of the finite absorbing area converges to that of infinite absorbing area described by the TMM. The reason for this phenomenon is the diffraction effect on the edges of the absorbing area. This effect is relatively larger when the source is higher, and it indicates that a closer source to the specimen is advantageous. Comparing three measurement techniques, the PU-method is also most stable against the effect of the absorbing area.

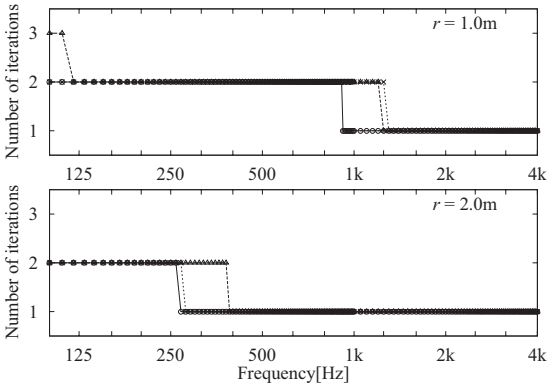

FIG. 7. Comparison on the number of iterations for the iterative determination algorithm calculated by the BEM: Γ is 1.0×1.0 m^2. —○—: the PU-method, ---△---: the PP-method, and ···×···: the UU-method.

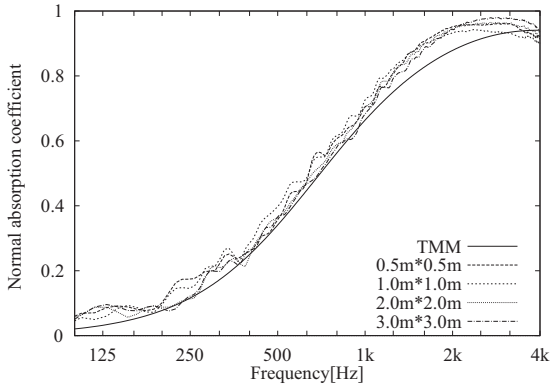

FIG. 9. Comparison of the normal absorption coefficients measured by the PU-method for different absorbing areas: $r=1$ m.

E. Number of iterations

The number of iterations is shown in Fig. 7 with respect to comparison of three measurement techniques. The upper side of the figure shows the number under the condition of $r=1.0$ m, the lower side of the figure shows the number under $r=2.0$ m, and the absorbing area is 1.0×1.0 m^2.

Since the longer distance r, the sound field around the receivers is closer to the plane-wave field, the number of iterations on $r=2.0$ m is less than those of $r=1.0$ m. The number for the PU-method is less than the others. On the other hand, the number for the PP-method in low frequency is more than the others in the case of $r=1.0$ m. Therefore, the convergence of the PU-method is faster than the others.

IV. EXPERIMENTAL INVESTIGATION OF THE PU-METHOD

A. Measurement procedure

The measurements described in the following were performed in a hemi-anechoic room. The dimensions of this hemi-anechoic room are the width of 4.8 m, the depth of 6.2 m, and the height of 3.6 m, and the cutoff frequency of the absorbing wedge is around 125 Hz. The sound was radiated by the full range loudspeaker with the diameter 13 cm (DIATONE DS-5). For improvement of signal to noise (S/N) ratio in low frequency, the sound source signal was used as the logarithmic swept sine signal,[19] and the impulse responses of the sound pressure and the particle velocity at PU-probe were measured. The raised cosine time window was applied to the impulse responses for elimination of unwanted reflected waves. Generating the sound signal, measuring the impulse responses, transforming into the frequency domain by fast Fourier transform, and postprocessing were processed by the personal computer.

The calibration of PU-probe was made by the free field calibration method.[10] It is shown that the acoustic impedance measured by PU-probe is corrected by the theoretical acoustic impedance in the free field. The measured normal absorption coefficient was smoothed by a moving average.

The measured porous material was a glass wool board with the thickness of 25 mm, the density of 98.5 kg/m^3, and the flow resistivity of 55 124 N s/m^4. This flow resistivity was measured by the method according to ISO 4638.[20]

B. Measurement results

Figure 8 shows comparison of the normal absorption coefficient calculated by the TMM, measured by the impedance tube with the diameter of 40 mm, and measured by the PU-method with $r=1$ m. Figure 10 shows the same comparison, however, for the PU-method with $r=2$ m. The infinite absorbing area for the PU-method was realized by spreading the material all over the floor in the hemi-anechoic room. The measured result by the PU-method corresponds to the measured value by the impedance tube and the calculated

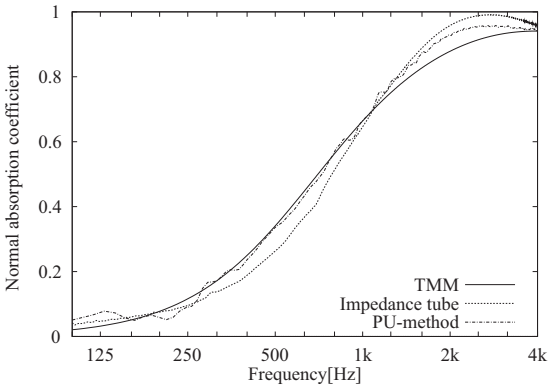

FIG. 8. Comparison of the normal absorption coefficients. The condition of "PU-method" is that $r=1$ m and the absorbing area is infinite.

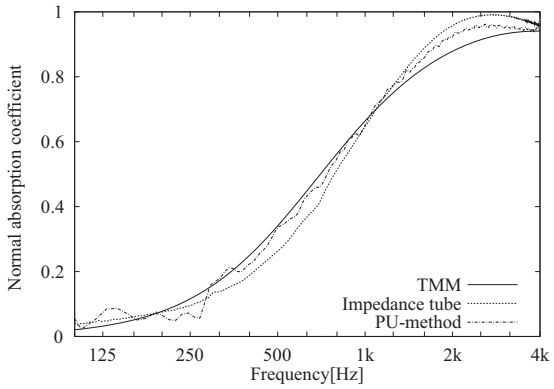

FIG. 10. Comparison of the normal absorption coefficients. The condition of "PU-method" is that $r=2$ m and the absorbing area is infinite.

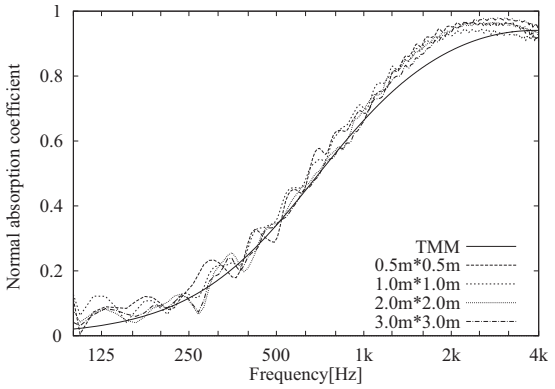

FIG. 11. Comparison of the normal absorption coefficients measured by the PU-method: $r=2$ m for different absorbing areas.

value by the TMM approximately in both cases of $r=1$ and 2 m. In other words, the TMM agrees with the measured values, and this shows that the numerical calculation has been verified by these results.

Figure 9 shows the normal absorption coefficient with different absorbing areas when $r=1$ m, and Fig. 11 shows that when $r=2$ m. As the BEM analysis of Fig. 5 points out, these figures indicate that the normal absorption coefficient measured by the PU-method is hardly changed by the different absorbing areas. The deviation of the measured normal absorption coefficient at frequencies lower than 300 Hz can be found, and the same deviation can also be found in the values calculated by the BEM. This deviation can be caused by the effects of absorbing areas and unwanted reflected waves. Since the absorption coefficient of a fibrous material at low frequencies is a small value, the normal component of the particle velocity close to the material becomes very small at those frequencies. Therefore, the effect of the diffracted waves from the material edges and the unwanted reflected waves to the receiver can be relatively bigger than that of the direct sound radiated from the sound source. Especially on this experiment, since the cutoff frequency of the absorbing wedges in this hemi-anechoic room is around 125 Hz, the reflected waves from the wedges may affect the measured values at low frequencies. Nevertheless, a larger absorbing area gives more stability to the normal absorption coefficient, and the value becomes closer to the TMM, because the effect of absorbing areas becomes small.

The deviation of the normal absorption coefficient with $r=1$ m is smaller than that with $r=2$ m, and this indicates that more stable measured values can be obtained by having the sound source closer to the specimen. In this study, the sound source, the loudspeaker with the diameter of 13 cm has been used, and it is not a real point source, even though the iterative determination algorithm premises the point source. If the loudspeaker is set close to the specimen, the measurement may lose the validity of the assumption. Therefore, it is important that the sound source regarded as the point source is used and the radiated sound is big enough to keep sufficient S/N ratio in low frequency.

V. CONCLUSIONS

In this study, three measurement techniques in the free field, which are the PU-method, the PP-method, and the UU-method, have been compared and discussed with the numerical analysis by the BEM and the experiment. The specimen used was a 25 mm glass wool and a locally reacting surface has been assumed, which is a reasonable assumption, given the high flow resistivity of the sample. As a result, following outcomes have been found.

- The PU-method is most stable against the effect of the absorbing area, and the UU-method is easily affected by that effect contrary to the original expectation.
- The major cause for variation in the normal absorption coefficient is the source height rather than the absorbing area. Because the source is higher, the direct source to receiver signal is relatively weaker compared to the effect from the diffraction of the edges. Therefore, a source closer to the specimen is advantageous for these measurement methods.
- The iterative determination algorithm works for the PU- and the UU-methods as well as the PP-method.
- The number of iteration of the PU-method is smaller than that of the PP- and the UU-methods.

In this study, since the loudspeaker with the diameter of 13 cm has been used for radiation of the sound in low frequency around 100 Hz, the loudspeaker could not be set very close to the specimen. If the loudspeaker realizing the ideal point source can be used, especially on the PU-method, more accurate measurement can be expected.

[1]ISO 10534, "Acoustics—Determination of sound absorption coefficient and impedance in impedance tubes—Part 1 and 2," (1998).
[2]T. E. Vigran, L. Kelders, W. Lauriks, P. Leclaire, and T. F. Johansen, "Prediction and measurements of the influence of boundary conditions in a standing wave tube," Acta. Acust. Acust. **83**, 419–423 (1997).
[3]U. Ingard and R. H. Bolt, "A free field method of measuring the absorption coefficient of acoustic materials," J. Acoust. Soc. Am. **23**, 509–516 (1951).
[4]T. M. Barry, "Measurement of the absorption spectrum using correlation/spectral techniques," J. Acoust. Soc. Am. **55**, 1349–1351 (1974).
[5]Y. Champoux and A. L'Espérance, "Numerical evaluation of errors associated with the measurement of acoustic impedance in a free field using two microphones and a spectrum analyzer," J. Acoust. Soc. Am. **84**, 30–38 (1988).
[6]J. F. Allard, Y. Champoux, and J. Nicolas, "Pressure variation above a layer of absorbing material and impedance measurement at oblique incident and low frequencies," J. Acoust. Soc. Am. **86**, 766–770 (1989).
[7]J. F. Allard and Y. Champoux, "In situ two-microphone technique for the measurement of the acoustic surface impedance of materials," Noise Control Eng. J. **32**, 15–23 (1989).
[8]J.-F. Li and M. Hodgson, "Use of pseudo-random sequences and a single microphone to measure surface impedance at oblique incidence," J. Acoust. Soc. Am. **102**, 2200–2210 (1997).
[9]H. de Bree, "An overview of microflown technologies," Acta. Acust. Acust. **89**, 163–172 (2003).
[10]R. Lanoye, G. Vermeir, W. Lauriks, R. Kruse, and V. Mellert, "Measuring the free field acoustic impedance and absorption coefficient of sound absorbing materials with a combined particle velocity-pressure sensor," J. Acoust. Soc. Am. **119**, 2826–2831 (2006).
[11]J. D. Alvarez and F. Jacobsen, "An iterative method for determining the surface impedance of acoustic materials in situ," in Proceedings of the Inter-Noise 2008 (2008).
[12]K. Hirosawa, H. Nakagawa, M. Kon, and A. Yamamoto, "Investigation of absorption coefficient measurement of acoustical materials by boundary element method using particle velocity and sound pressure sensor in free field," Acoust. Sci. & Tech. **30**(6), 442–445 (2009).

[13]U. Ingard, "On the reflection of a spherical sound wave from an infinite plane," J. Acoust. Soc. Am. **23**, 329–335 (1951).
[14]M. A. Nobile and S. I. Hayek, "Acoustic propagation over an impedance plane," J. Acoust. Soc. Am. **78**, 1325–1336 (1985).
[15]T. Terai, "On calculation of sound fields around three dimensional objects by integral equation methods," J. Sound Vib. **69**, 71–100 (1980).
[16]Y. Kawai and H. Meotoiwa, "Estimation of the area effect of sound absorbent surfaces by using a boundary integral equation," Acoust. Sci. & Tech. **26**, 123–127 (2005).
[17]J. F. Allard and Y. Champoux, "New empirical equations for sound propagation in rigid frame fibrous materials," J. Acoust. Soc. Am. **91**, 3346–3353 (1992).
[18]B. Brouard, D. Lafarge, and J. F. Allard, "A general method of modelling sound propagation in layered media," J. Sound Vib. **183**, 129–142 (1995).
[19]T. Fujimoto, "A study of tsp signal getting higher sn ratio at low frequency bands," in Proceedings of the 1999 Autumn Meeting of Acoustical Society of Japan, pp. 433–434, in Japanese.
[20]ISO 4638, "Polymeric materials, cellular flexible—Determination of air flow permeability," (1984).